Effect of ketamine on early synaptic mistuning and emotional behavior deficits in App^{NL-F} mouse model of Alzheimer's disease.

Benjamin Portal[1, *], Moa Södergren[1], Teo Parés i Borrell[1], Nicole Metzendorf[2], Greta Hultqvist[2], Per Nilsson[3], Maria Lindskog[1, 3]

1. Department for Medical Cell Biology, Uppsala University, Uppsala, Sweden
2. Department of Pharmacy, Division of Protein Drug Design, Uppsala University, Uppsala, Sweden
3. Department of Neurobiology, Care Sciences and Society, Division of Neurogeriatrics, Center for Alzheimer Research, Karolinska Institutet, Stockholm, Sweden

* **Corresponding author**:
Benjamin Portal
Uppsala University
Department for Medical Cell Biology
Box 571
751 23 Uppsala
Sweden
Email: Benjamin.Portal@uu.se

ABSTRACT

Alzheimer's disease is the most common neurodegenerative disease, reported as 75 to 80% of dementia cases worldwide. Unfortunately, there are to date no disease modifying treatments available for this mental illness. It is therefore urgent to identify new pharmacological targets. Alzheimer's disease is thought to be caused by important phosphorylation of the microtubule associated protein Tau and abnormal amyloid-beta (Aβ) accumulation around brain cells, together causing neurodegeneration. Whether the late phases of the disease are well described, recent evidence suggest synaptic impairments at a pre-Aβ plaque stage. However, the underlaying mechanisms remain yet to be clarified. In this study we used the App^{NL-F} knock-in mouse model of Alzheimer's disease which carries two disease-causing mutations inserted in the amyloid precursor protein (App) gene and shows pathological Aβ plaques not earlier than fifteen months of age. To better understand early changes, we investigated in six months old animals, synaptic plasticity, and its potential pharmacological targeting in the treatment of this pathology. Our electrophysiological recordings revealed an overall synaptic mistuning at a pre-plaque stage of the pathology, associated to an intact social memory but a higher apathy-like and depression-like behavior. Interestingly, a single injection of ketamine (5mg/kg), twenty-four hours prior to experiment, partially corrected synaptic and depression-like behavior observed in six months old animals, compared to non-treated controls. In contrast with the amyloid-hypothesis of Alzheimer's disease, our study shows that earlier synaptic impairments could at least in part be the cause of the later-on observed symptoms, which could be prevented by pharmacological intervention.

KEY WORDS: Alzheimer's disease; Depression; Early stages; Synaptic tuning; Pharmacology

1. INTRODUCTION.

Alzheimer's disease is a progressive age-related neurodegenerative disorder accounting for 75% of dementia cases worldwide [1]. Patients show significant memory loss [2] and multiple secondary symptoms such as social isolation [3] and depressive symptoms [4]. In recent years, significant improvements have been done in clinical care of patients; However, the underlaying mechanisms of this pathology remain to be clarified.

The intracellular Tau neurofibrillary tangles [5] and the amyloid-beta (Aβ) aggregation [6] are the molecular hallmarks of the pathology, and are generally believed to cause synaptic changes [7]. Several studies have pointed out synaptic plasticity (i.e., neuronal adaptation, functional or morphological following an external stimulation, [8]) impairments, suggested to accelerate the neurodegeneration [9] and cause important memory loss [10]. Moreover, clusters of hyperexcitable neurons have been identified nearby Aβ plaques [11], most likely due to passive and active neuronal electrical properties changes [12].

However, the amyloid origin of the pathology is controversial [13] as the memory loss observed in Alzheimer's patients does not necessarily correlate with the number of amyloid plaques. Meanwhile, recent work clearly shows impairments in neuronal function as well as behavior well before detection of plaques [14]. Amyloid misprocessing leads to many Aβ products, including Aβ oligomers, proposed to be the most toxic for neurons [15]. This is in good agreement with clinical data showing that neurobiological changes can occur up to twenty years before the appearance of the first memory deficits [16]. It is therefore important to better understand early changes (i.e., before Aβ plaques) for diagnosis and treatments. Alzheimer's disease is also associated to a loss of synaptic plasticity and a progressive reduction in the number of synapses. Importantly, recent work suggests that impairment in synaptic transmission occur long before occurrence of Aβ accumulation [17], and that a deficit in neuronal activity set-point may be an underlaying mechanism of the pathology [18].

Early symptoms of Alzheimer's disease reach beyond memory loss. Among others, neuropsychiatric disorders (e.g., sleep disturbance, psychosis, also defined as delusion and hallucination, [19]), apathy (i.e., lack of interest) and affective syndromes (e.g., depression and anxiety) [20] are common and even used as elements of diagnosis for Alzheimer's disease.

70 Until recently, there were no disease modifying treatments although recent anti-Aβ immunotherapies
71 have shown promising results in early phases of the pathology [21, 22]. Nevertheless, we need new
72 strategies to better treat Alzheimer's disease. To do so, many animal models have been engineered
73 [23], yet none of them recapitulate all the symptoms of the pathology. One common feature is an
74 important Aβ accumulation [24] already at a young age, hampering the study of pre-plaques phases.
75 Only a few preclinical studies have focused on the development of early symptoms in Alzheimer's
76 disease. For example, Arroyo-Garcia and colleagues revealed synaptic impairments in an App
77 knock-in mouse model [25]; Loera-Valencia and colleagues have shown an impaired synaptic
78 plasticity in a hypercholesterolemia mouse model of Alzheimer's disease [26].
79 The App^{NL-F} mouse line is a late onset knock-in model of Alzheimer's disease, interesting to
80 study early stages of the pathology. This model carries two disease causing mutations (the Swedish
81 mutation, NL and the Beyreuther/Iberian mutation, F) in the amyloid precursor protein (App) gene
82 [24] and does not develop pathological plaques until fifteen months of age [27], giving a very large
83 window to explore pre-plaques stages. While no Tau pathology has been unveiled in this model [28]
84 many molecular changes such as autophagy disturbances [29] and mitochondria dysfunctions [30]
85 were reported both *in vivo* and *in vitro*. Interestingly, early Wnt pathway disruption, known to be
86 crucial for synaptic activity [31], has been pointed out in the cortex of six months old App^{NL-F} animals
87 [14], strongly suggesting early synaptic impairment in this model.
88 In the present study we identify early synaptic changes in this App knock-in mouse model
89 App^{NL-F}. Electrophysiological recordings revealed a reduced excitatory synaptic activity and altered
90 plasticity, associated to an increased depression-like behavior. We show that these early alterations
91 can be partially corrected by a low dose of the N-methyl-D-aspartate (NMDA) receptors antagonist
92 ketamine, delivered twenty-four hours prior to experiment
93
94 **2. METHODS.**
95 *2.1. Animals.*
96 App^{NL-F} mice model of Alzheimer's disease were bred locally at Uppsala University. These mice
97 carry the Swedish (KM670/671NL) and the Beyreuther/Iberian (I716F) mutations in the App gene
98 [24, 27]. Age-matched C57Bl6 mice were bought from Charles River (Germany). Both strains were

housed in the same conditions, on a 12:12 light-dark cycle and with access to food and water *ad libitum*. All experiments were conducted in six months old males.

2.2. Drugs.

Ketamine (Ketaminol® vet., 100 mg/kg, Intervet) was diluted in vehicle solution (natriumchloride, NaCl 0.9%) and delivered intraperitoneally (i.p.; 5 mg/kg) twenty-four hours prior to experiments. Tetrodotoxin (TTX; Tocris 4368-28-9) was diluted in artificial cerebrospinal fluid (aCSF) and used in patch-clamp experiments at a concentration of 1 μM.

2.3. Behavioral Analysis.

Animals were habituated to the experimental room twenty minutes prior to experiments. The luminosity of the room was set on 30 lux and the temperature at 21°C ± 1°C.

To characterize the App^{NL-F} model, three cohorts of mice were used for the following sets of behavior tests:

- Cohort 1: Open field test, five-trials social memory test and olfactory habituation/dishabituation,
- Cohort 2: Elevated plus maze, splash test, forced swim test and sucrose preference test,
- Cohort 3: Splash test and forced swim test

In the ketamine experiments, two cohorts were used:

- Cohort 1: Five-trials social memory test, open field and forced swim test,
- Cohort 2: Five-trials social memory test, open field, Splash test and elevated plus maze,

The tests were performed in the described order, with at least three days between each test. For the ketamine treatments, ketamine was given twenty-four hours before each test.

2.3.1. Five-trials social memory test.

The mice were habituated to an empty square arena (50cm x 50cm) for ten minutes, followed by five minutes exploration of the same arena with an empty removable cage (8cm x 8 cm x 9 cm). An unknown mouse (same genotype, same fur color, same age, and same gender as the test mouse)

was placed for five minutes in the removable cage for four consecutive trials, separated with ten minutes. One hour after the fourth trial, a new unknown mouse was placed in the cage for five minutes. Social interactions were manually scored.

2.3.2. Olfactory habituation/dishabituation test.

The mice were isolated in individual standard cages in which they performed the whole experiment and habituated for at least twenty minutes. Cotton swabs soaked with non-social odors (melon and banana) or social odors (one form their home cage, one from a non-familiar cage) were presented to the animal for two minutes. Each odor was presented three times.

2.3.3. Open field test.

The animals were free to explore a spatial-cue-free square arena (50cm x 50cm) for ten minutes. The central zone and peripheral zone were defined in the Ethovision software (Noldus tech, The Netherlands). The area of the central zone was defined as 50% of the area of the arena. The total travelled distance, the time spent in the central area, as well as the number of entries in the central zone, were automatically analyzed by the software.

2.3.4. Elevated plus maze.

The maze was composed of two open arms, two closed arms, linked together at a central platform and positioned 50 cm above ground. Mice were placed on the central platform facing one open arm and were let to explore for five minutes. The number of entries and the time spent in the open arms were manually scored. An animal was considered "in the arm" when the four paws crossed the virtual line between the central platform and the considered arm.

2.3.5.Splash test.

The animals were isolated in a new cage and habituated for at least twenty minutes. The test was performed as previously described [32]: 200 µL of 10% sucrose solution was squirted on the mouse's snout and the grooming behavior (latency to first, frequency and total time), used to evaluate

155 self-care, was manually scored for five minutes. Mice were placed back together in their home cage
156 after the experiment.
157
158 2.3.6. Forced swim test.
159 The mice were placed in a cylinder (30 cm high, ∅ 18 cm) filled with 25 ± 1°C water to a
160 height of 17 cm where no part of the animal could touch the bottom. The mice were left in the cylinder
161 for six minutes, and the time spend immobile was quantified during the last four minutes. Latency to
162 first immobility and the total time of immobility were manually scored. An animal was considered as
163 immobile when it was floating and none of the paws nor the tail was moving.
164
165 2.3.7. Sucrose preference test.
166 Each animal was singled housed and habituated to drink water from two identical bottles for forty-
167 eight hours. During the following seventy-two hours, mice could choose between water and a 1%
168 sucrose solution. Sucrose solution intake was measured by weighting the bottles before and after
169 the last twenty-four hours and expressed as the percentage of the total amount of liquid ingested,
170 normalized to the mouse body weight. Each bottle was replaced and switched from left to right daily.
171
172 *2.4. Emotionality z-score.*
173 Z-normalization was used in this study as a complementary measurement for emotionality-
174 related behavior, obtain from different paradigms [33]. Raw behavioral data (parameters of interest)
175 were normalized to the control group using the following equation $z = (X - \mu)/\sigma$ with X being the
176 individual value for the considered parameter, μ being the mean of the control group and σ being
177 the standard deviation of the control group. Each parameter of interest gave a parameter z-score
178 (zSC_param), adjusted so that an increased score reflects an increased emotionality. For each test,
179 all parameter scores were averaged into a test score (zSC_test), and eventually averaged to give
180 an individual emotionality z-score.
181 More details about the exact list of parameters of interest and the mathematical method are available
182 in **supplementary table 1 and 3**.

183 *2.5. Electrophysiology.*

184 2.5.1. Brain slicing.

185 For the preparation of acute slices, mice were anesthetized with isofluorane and decapitated
186 soon after the disappearance of corneal reflexes. 300 µm thick horizontal sections were prepared
187 using a Leica VT1200 vibrating microtome (Leica Microsystems, Nussloch, Germany) in dissection
188 solution containing 250 mM sucrose, 2.5 µM KCl, 1.4 mM NaH_2PO_4, 26 mM $NaHCO_3$, 10 mM
189 glucose, 1 mM $CaCl_2$ and 4 mM $MgCl_2$, and bubbled with carbogen gas (5% CO_2, 95% O_2).
190 Hippocampi were dissected and slices were placed in a recovery chamber filled with aCSF
191 containing (in mM): 130 NaCl, 3.5 KCl, 1.25 NaH_2PO_4, 24 $NaHCO_3$, 10 glucose, 2 $CaCl_2$ and 1.3
192 $MgCl_2$ and bubbled with carbogen gas.

193

194 2.5.2. Patch clamp recording.

195 After a recovery period of at least two hours, slices were transferred in a submerged recording
196 chamber with a perfusion rate of 2-3 mL per min with standard aCSF, tempered at 32 ± 1°C and
197 bubbled with carbogen gas. Borosilicate glass pipettes with a tip resistance of 4-5 MΩ were used for
198 patching neurons. The glass pipettes were filled with a solution containing (in mM) 110 K-gluconate,
199 10 KCl, 4 Mg-ATP, 10 Na_2-phosphocreatine, 0.3 Na-GTP, 10 4-(2-hydroxyethyl)piperzine-1-
200 ethanesulfonic acid (HEPES) and 0.2 ethylene glycol tetraacetic acid (EGTA) (pH 7.2-7.4; 270-290
201 mOsm). Pyramidal neurons were identified by shape and localization in stratum radiatum of area
202 CA1 of the hippocampus. Spontaneous Excitatory Post-Synaptic Currents (sEPSC) were recorded
203 in absence of any drugs, whereas miniature Excitatory Post-Synaptic Currents (mEPSC) were
204 recorded in the presence of 1 µM TTX.
205 The access resistance was monitored throughout the recordings and data were included only for
206 stable values (< 30% variation). The signal was acquired using an Ag/AgCl electrode connected to
207 a Multiclamp 700B amplifier, digitized with Digidata 1440A and handled with the Clampex software
208 (v. 10.0; Molecular Devices).

209 Traces were analyzed using the Easy electrophysiology software (v. 2.4). The event
210 detection was based on a template fitting method. Probe recordings (three recordings of one minute
211 each) from C57Bl6 wild type acute hippocampus slices were used to generate and refine a template

212 from representative events corresponding to an average of ten to twenty detected EPSC. Event
213 detection in App^{NL-F} and C57Bl6 controls acute slices was then run on a semi-automatic method:
214 each event detected fits the previously generated template. A minimum amplitude threshold of 10
215 pA was applied: all events that were detected between 0 pA and 10 pA were discarded. Each
216 recording was analyzed on a period of 1 minute.
217
218 2.5.3. Field recording.
219 After a recovery period of at least two hours, slices were transferred in a submerged recording
220 chamber with a perfusion rate of 2-3 ml per min with standard aCSF, tempered at 32±1 °C and
221 bubbled with carbogen gas. An extracellular borosilicate recording pipette filled with aCSF was
222 placed in the stratum radiatum of area CA1 and field Excitatory Post-Synaptic Potentials (fEPSP)
223 were evoked by electrical stimulation of the Schaffer collaterals using a bipolar concentric electrode
224 (FHC Inc., Bowdoin, ME), connected to an isolated stimulator (Digitimer Ltd., Welwyn Garden City,
225 UK). Recordings were performed with the stimulus intensity to elicit 30-40% of the maximal response
226 and individual synaptic responses were evoked at 0.05 Hz (every 20 seconds). The acquired signal
227 was amplified and filtered at 2 kHz (low-pass filter) using an extracellular amplifier (EXT-02F, NPI
228 Electronic, Tamm, Germany). Data were collected and analyzed using a Digidata 1440A, Axoscope
229 and Clampfit softwares (Molecular Devices, San Jose, CA). Responses were quantified by
230 determining the slope of the linear rising phase of the fEPSP (from 10% to 70% of the peak
231 amplitude). The response was normalized to the average baseline measured in the last ten minutes
232 prior to the start of the experiment.
233 To study long term synaptic plasticity, we used ten theta-bursts (θ-burst) separated with 200
234 ms. Each θ-burst is four pulses at 100 Hz, a stimulation protocol tested not to be enough to trigger
235 Long Term Potentiation (LTP) in slices from C57Bl6 mice.
236

237 *2.6 Western blot.*

238 2.6.1 Structure dissection.

239 Mice were anesthetized with isofluorane and decapitated soon after the disappearance of
240 corneal reflexes. The brain was extracted, hippocampus rapidly dissected in ice, frozen on dry ice
241 and kept at -80°C until protein extraction.

242

243 2.6.2 Protein extraction, Migration and Analysis.

244 Hippocampi were homogenized in a lysis solution containing RIPA buffer, phosphatase
245 inhibitors (ThermoFisher A32957) and protease inhibitors (ThermoFisher A32953). Samples were
246 diluted in LDS sample buffer (ThermoFisher NP0007) and an equal amount of protein (20 µg) was
247 loaded onto a NuPAGE™ 4-12% Bis-Tris gel (ThermoFisher NP0336BOX), run four hours at 80V
248 and transferred (2h at 80V) to a PVDF membrane.

249 Membranes where blocked with 5% BSA+ 5% Normal Donkey Serum, incubated with primary
250 antibodies overnight and then with the appropriate secondary antibodies. The fluorescent signal was
251 visualized using the LiCOR Odyssey infrared detection system (Lincoln, Ne, USA). The amount of
252 fluorescence for each band was quantified with FIJI software (v. 2.9 NIH, Bethesda, MD, USA).
253 GAPDH was used as the loading control protein

254 A full list of the used antibodies and their concentration is available in **supplementary table 5**.

255

256 2.7 *Immunohistochemistry.*

257 2.7.1 Perfusion and brain extraction.

258 Mice were deeply anesthetized with a mixture of ketamine (100 mg/kg) and xylazine (16
259 mg/kg) i.p. In absence of corneal reflexes, mice were transcardially perfused with NaCl 0.9%
260 followed by a 4% PFA solution. The brain was extracted and post-fixed in a 4% PFA solution for
261 forty-eight hours, washed in PBS for twenty-four hours and placed in a 30% sucrose + 1% natrium
262 azide solution until further use.

263

264 2.7.2 Slicing and staining.

265 The brains were sliced in 40 µm thick sections using a cryostat (Thermo Scientific Cryostar
266 NX70) tempered at 4°C. Free-floating slices were treated with a 10% formic acid solution for ten
267 minutes for epitope retrieval. After blocking steps with normal donkey serum, slices were incubated
268 with primary Aβ antibody (Covence Signet SZG-39300-200; 1:5000) overnight at 4°C and then with
269 Alexa fluor Donkey anti-mouse 647 (1:5000; Invitrogen A31571) for two hours. DAPI (1:5000) was
270 added to counterstain nuclei. Slices were then mounted on non-coated microscope glass coverslips
271 using the fluoromount mounting medium (Invitrogen, 00-4958-02).
272 Images were taken on a confocal microscope (Zeiss LSM700) with a 10x objective and the Zeiss
273 Zen software was used during the whole imaging process.
274

275 *2.8 Amyloid-beta (Aβ) ELISA.*

276 2.8.1 Perfusion and brain extraction.

277 Mice were anesthetized with a mixture of ketamine (100 mg/kg) and xylazine (16 mg/kg)
278 administered via i.p route. In absence of corneal reflexes, mice were transcardially perfused with
279 NaCl 0.9%. The brain was extracted, and hippocampi, cortex, and cerebellum were dissected in dry
280 ice and kept at -80°C until further use.
281

282 2.8.2 Brain homogenization.

283 The brain regions were homogenized at 1:5 weight/volume ratio in precellys homogenization
284 tubes (Bertin Technologies, P000933-LYSK0-A). A three-step homogenization was applied: Tris-
285 buffered saline (TBS) to isolate soluble Aβ, TBS with 1% triton-x100 (TBS-T; Sigma-Aldrich, X100)
286 for isolation of membrane-associated Aβ, and 70% (v/v) formic acid (FA; Sigma-Aldrich, F0507) for
287 the insoluble Aβ fraction. TBS-homogenized brains were centrifuged at 16 000 x g for sixty minutes
288 at +4°C, the supernatant was collected. The pellets were subsequently homogenized in TBS-T and
289 centrifuged at 16 000 x g for sixty minutes at +4°C and supernatant was collected. The pellets were
290 dissolved in 70% (v/v) FA, centrifuged at 16 000 x g for sixty minutes at +4°C and the supernatant
291 was collected and immediately neutralized with 1M Tris pH 8.0 (Thermo Fisher Scientific, AM9856).
292

293 2.8.3 Aβ ELISA.

294 The three Aβ fractions were analyzed using a homogenous sandwich ELISA using the Aβ
295 N-terminal specific antibody 3D6 (murine version of Bapineuzumab, produced in-house) as both
296 capture and detection antibody. 96-wells ELISA plates were coated with 1 µg/mL 3D6 and
297 incubated over night at +4°C. Plates were blocked with 1% (w/v) BSA in PBS 1X for two hours.
298 Dilutions of TBS and TBS-T brain fractions (1:10 (v/v)) and FA brain fraction (1:200 (v/v)) in
299 ELISA incubation buffer (EIB; 0.05% tween-20 (Sigma-Aldrich, P9416), 0.1% w/v BSA in PBS
300 1X) were added to the ELISA plate and incubated over nigh at +4°C. Biotinylated 3D6 (prepared
301 in-house; 1 µg/mL in EIB) was incubated for two hours at room temperature followed by one hour
302 of streptavidin-HRP (Mabtech, 3310-9-1000) at room temperature. The ELISA was developed
303 with K-blue Aqueous TMB substrate (Neogen Corp., 331177) and read with a spectrophotometer
304 (Tecan, Spark) at 450 nm.

305

306 *2.9 Statistical analysis.*

307 IBM SPSS Statistics (v. 28 IBM corp) was used to perform the statistical analysis. For each
308 experiment, a Shapiro-Wilk test for normality and Levene's test for homogeneity of variances were
309 used to determine the subsequent test to compared means. For all the tests, 0.05 was set as the
310 significance threshold. All results are shown as mean ± S.E.M.

311 A summary of statistics is available in **supplementary table 2 and 4.**

312

313 **3. RESULTS.**

314 *3.1. App^{NL-F} mice show no plaques but increased insoluble Aβ at six months old.*

315 One of the common features of Alzheimer's disease animal models is the over App
316 degradation, leading to an early increased concentration of Aβ. Likewise, it is generally accepted
317 that such phenomenon can initiate an important aggregation resulting in neuronal impairments. As
318 previously described, Aβ plaques in the hippocampus of App^{NL-F} mouse model are not detectable
319 with immunohistochemistry before twelve months, with a very high load at fifteen months of age. Aβ
320 immunostaining in the hippocampus of six months old animals confirmed the absence of plaques
321 (**figure 1A**). To investigate whether Aβ accumulation can occur before plaques detections, we

322 performed an ELISA immunoassay that detects aggregated Aβ (larger than dimers). Interestingly,
323 our analysis revealed an increase in the relative amount of membrane-bound Aβ aggregates (as
324 found in the TBST fraction) in the hippocampus App^{NL-F} mice compared to C57Bl6 ($p<0.001$, with no
325 difference in the cortex nor the cerebellum, **figure 1C**). Moreover, non-soluble Aβ (e.g., plaques, as
326 found in the formic acid fraction) was increased in both the cortex ($p<0.01$) and the hippocampus
327 ($p<0.01$) but not in the cerebellum (**figure 1D**). No differences in the relative concentration of non-
328 membrane-bound Aβ oligomers (as found in the TBS fraction) were unveiled in any of the three-
329 brain regions (**figure 1B**).
330 Thus, even though the level of App is similar between App^{NL-F} and C57Bl6 mice [24], and the
331 absence of large plaques, we show Aβ accumulation in the hippocampus of six months old App^{NL-F}
332 animals, consistent with previous observations *in vitro* [34].We hypothesize that this can lead to
333 subsequent neuronal dysfunctions.
334

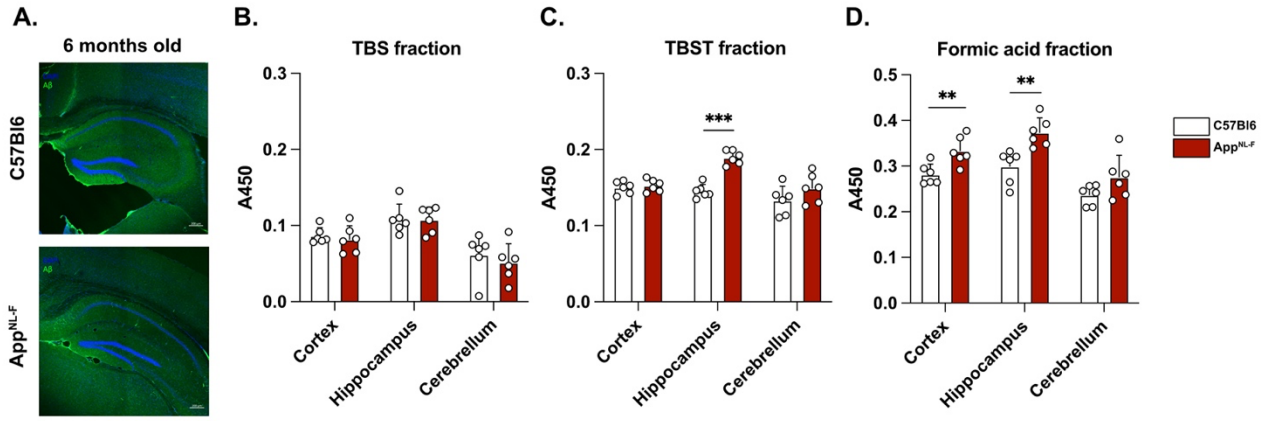

<u>Figure 1</u> : ***App^{NL-F} mice do not display Aβ plaques but higher insoluble fraction in the hippocampus.***

Immunolabelling of Aβ (A.) reveals the absence of plaques in the hippocampus of six months old App^{NL-F} mice, compared to C57Bl6 mice. ELISA analysis of different Aβ fractions shows unchanged concentrations in non-membrane-bound Aβ (TBS fraction, B.) in the hippocampus, the cortex and the cerebellum. However, increased concentration in membrane-bound Aβ (TBST fraction) in the hippocampus (C.) but not in the cortex nor the cerebellum were observed. Our analysis also revealed an increased formic acid fraction (i.e., non-soluble dimers) in both the cortex and the hippocampus (D.).

*For the three fractions: Two-way ANOVA with the genotype and the brain region as the main factors. Bonferroni multiple comparison: **, $p<0.01$; ***, $p<0.001$ statistically significant as shown. C57Bl6: n=6, App^{NL-F}: n=6. Figure A: scale bar 200µm.*

350 *3.2. Glutamatergic synapses' activity is reduced in area CA1 at six months old App^{NL-F} mice.*

351 Whole-cell patch clamp technique (**figure 2A**) in glutamatergic neurons in the stratum radiatum
352 of area CA1 of the hippocampus showed that resting membrane potential (**figure 2B**) was
353 significantly higher ($p<0.05$) in App^{NL-F} mice (-51.74 ± 1.32 mV) compared to C57Bl6 mice (-56.18 ±
354 1.38 mV), suggesting impaired neuronal functions. Spontaneous synaptic activity in active
355 hippocampal network (sEPSC) was not different between the two strains in neither frequency
356 (C57Bl6: 0.37 ± 0.12 Hz, App^{NL-F}: 0.25 ± 0.06 Hz; **figure 2C, G**) or amplitude (C57Bl6: -29.94 ± 1.96
357 pA, App^{NL-F}: -28.20 ± 1.93 pA; **figure 2D**). Decay and rise time of sEPSC were also unchanged
358 between genotypes (**supplementary figure 1A, B**). However, when action potentials were blocked
359 with the sodium channel blocker TTX (1 μM), allowing us to record spontaneous release of individual
360 synaptic vesicles (mEPSC) we observed a reduced frequency of the mEPSC (**figure 2E, G**) in App^{NL-}
361 ^{F} mice (0.27 ± 0.04 Hz) compared to C57Bl6 mice (0.56 ± 0.08 Hz; $p<0.01$), whereas the amplitude
362 (C57Bl6: -21.71 ± 1.48 pA, App^{NL-F}: -19.65 ± 1.43 pA) remained unchanged (**figure 2F**). No
363 differences were unveiled in the to decay and rise time of mEPSC (**supplementary figure 1C-D**
364 respectively). These observations revealed the presence of dysfunctional synapses in App^{NL-F}
365 animals already at six months old.
366

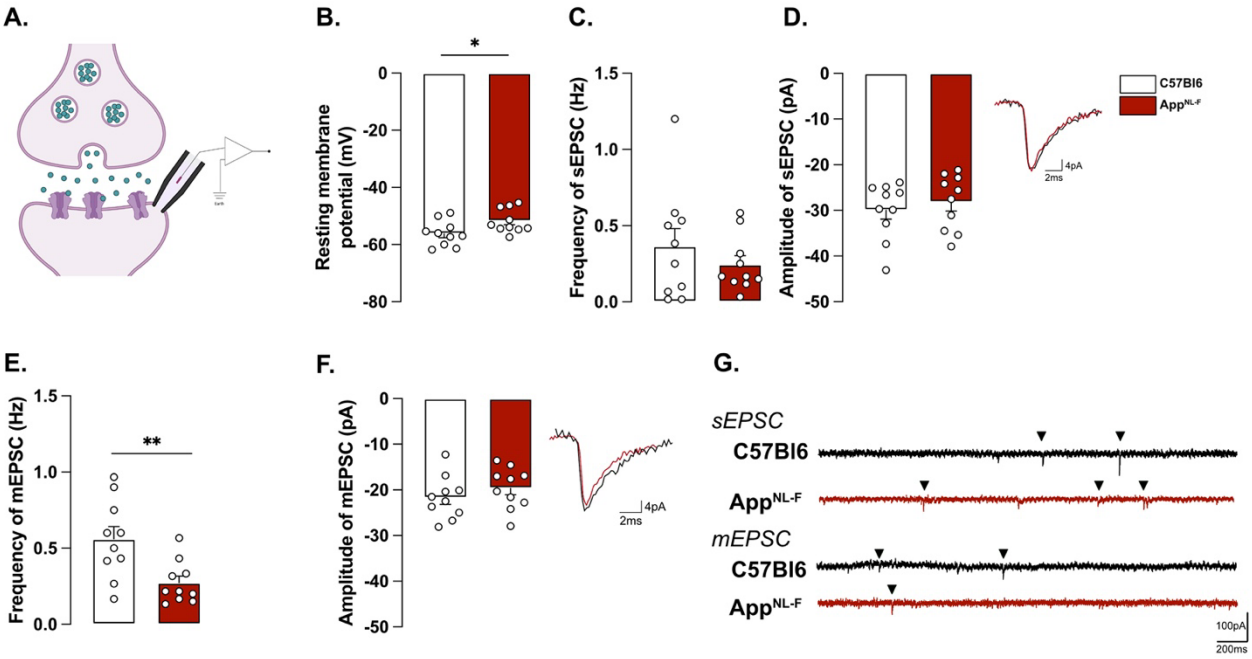

<u>Figure 2</u> : Area CA1 glutamatergic neurons' activity is impaired in App^{NL-F}

*Patch clamp experiment (A.) reveales a higher resting membrane potential in App^{NL-F} mice compared to C57Bl6 mice (B.). Although the frequency (C.) or the amplitude (D.) of sEPSC is unchanged, the frequency of mEPSC (E.) is significantly reduced in App^{NL-F}. Interestingly, the amplitude of these mEPSC (F.) remains unchanged. (G.) depicts representative traces for both sEPSC and mEPSC. Student t-test *, p<0.05, **, p<0.01 statistically significant as shown. For all variables, C57Bl6: n=10 cells recorded in seven animals, App^{NL-F}: n=10 cells recorded in seven animals.*

377 *3.3. Glutamatergic synapses in area CA1 are more sensitive.*

378 Based on previous observations of our lab [35], we hypothesize that synapses could be mistuned
379 at the cost of an impaired plasticity. Thus, the possibility to undergo long-term potentiation (LTP) was
380 examined, using a subthreshold stimulation protocol that did not evoke LTP in C57Bl6 mice (**figure**
381 **3A**). Ten theta-bursts (θ-burst) stimulation of Schaffer collaterals induced an immediate potentiation
382 of synaptic strength, as measured as the increased slope of the evoked fEPSP, in both genotypes
383 ($p<0.001$; **figure 3B, C**) However, after one hour, the fEPSP had progressively returned to baseline
384 in control animals, whereas the magnitude of the fEPSP was still significantly increased in App^{NL-F}
385 mice ($p<0.001$ different from the baseline; **figure 3D**), suggesting an increased synaptic plasticity.

386 To molecularly characterize these observations, we assessed glutamate-pathway related protein
387 expression in whole hippocampus protein extracts with western-blot. The NMDA receptor GluN2A
388 subunit was significantly increased in App^{NL-F} extracts compared to C57Bl6 extracts (~ 2.5-fold
389 increase, $p<0.05$) while no difference was observed in the levels of the GluN1 or GluN2B subunits
390 (**figure 3E**). No significant difference was observed in the assessed signaling proteins involved in
391 LTP: CamKII (α and β subunits) and ERK1/2, nor it's phosphorylated version p-ERK (**figure 3F**). An
392 increased levels of GluN2A subunit, believed to be the most dynamic in the LTP phenomenon [36],
393 is in good agreement with the reduced threshold for LTP.

394

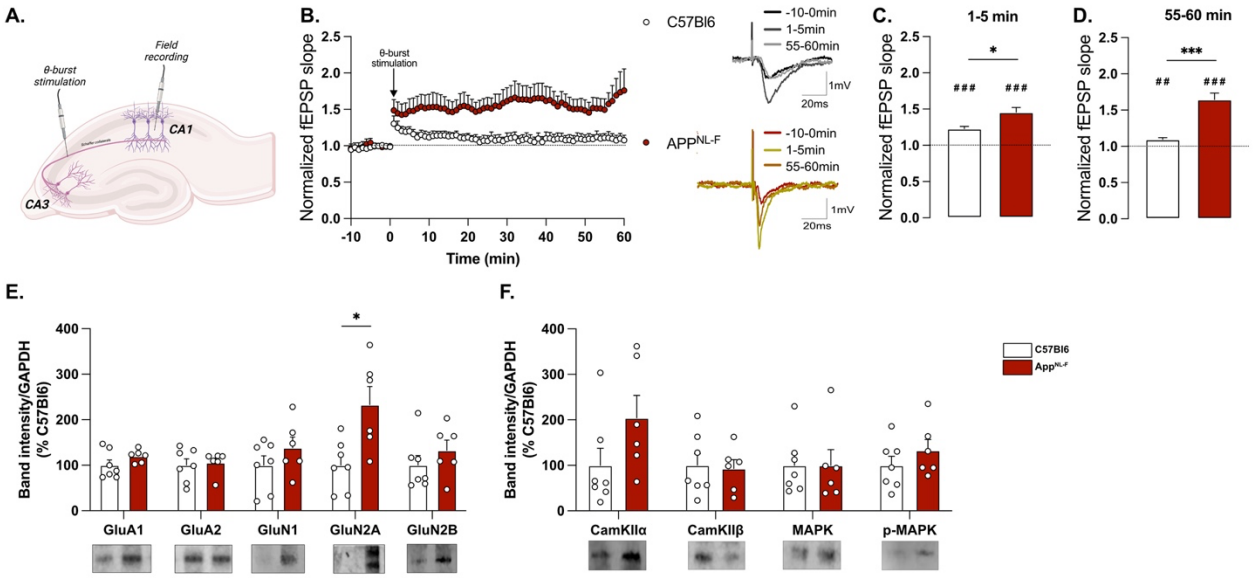

395

396 ***<u>Figure 3</u> : Synaptic mistuning is associated with an increased expression of NMDA receptors.***

397 *After Schaffer collaterals stimulation, we recorded the response of post-synaptic neurons in area*
398 *CA1 of the hippocampus (H.). After ten minutes of baseline recording, we applied a customized θ-*
399 *burst stimulation protocol and follow the response up to one hour after the stimulation (I.). Our*
400 *protocol potentiates the fEPSP (J.) which, after one hour is almost back to the baseline values (K.)*
401 *in C57Bl6 mice. Interestingly, the stimulation triggers a long-term potentiation (LTP) in six months*
402 *old App^{NL-F} animals, revealing early higher synaptic sensitivity. Student t-test: ##, p<0.05, ###,*
403 *p<0.001 statistically significant from 1; Student t-test: *, p<0.05, ***, p<0.001 statistically significant*
404 *as shown. C57Bl6: n=6 recordings in three animals, App^{NL-F}: n=9 recordings in five animals.*
405 *Using western-blot analysis, we identified an increased expression of NMDA receptors subunit 2A*
406 *in the hippocampus of App^{NL-F} mice (E.). The expression of the other NMDA receptors subunits, the*
407 *different AMPA receptors subunits as well as downstream molecular actors (F.) were unchanged.*
408 *Mann-Whitney test **, p<0.01 statistically different as shown. C57Bl6 controls: n=7, App^{NL-F}: n=6*
409

410 *3.4. App^{NL-F} mice show no social memory impairments but a lack of motivation.*

411 Six months old App^{NL-F} mice have no spatial memory impairments [37], although our
412 electrophysiological and molecular results suggest a dysfunction of the hippocampal network already
413 at this age. Social memory problems have been pointed out in other relevant transgenic mice model
414 of Alzheimer's disease [38], consistent with early social isolation and poor social recognition in
415 patients [39]. We therefore asked whether six months old App^{NL-F} mice present social memory
416 problems. This possibility was explored in the five-trials social memory test in which during four
417 consecutive trials the social interactions with an unknown animal is used to evaluate social memory
418 whereas the interaction with a new animal on the fifth trial is used to assess the motivation (**figure**
419 **4A**). A similar decrease in social interactions was observed over the four first trials in both App^{NL-F}
420 and C57Bl6 animals (**figure 4B, C**), suggesting no social memory impairments at six months old.
421 Whilst on the fifth trial social interactions with a new animal were increased in control mice (27.38 ±
422 9.14% on trial 4 vs. 87.11 ± 9.18% on trial 5; **figure 4B-C**), they were similar to the one observed in
423 the fourth trial in App^{NL-F} mice (34.94 ± 6.33% on trial 4 vs. 42.03 ± 13.62% on trial 5). Furthermore,
424 the latency to first interaction was similar in both groups during the first trial, (C57Bl6: 26.32 ± 13.31
425 seconds, App^{NL-F}:11.69 ± 6.903 seconds), however it was significantly increased in App^{NL-F} mice
426 compared to C57Bl6 controls (**figure 4D**; $p<0.01$) on the fifth trial (C57Bl6: 9.73 ± 5.13 seconds,
427 App^{NL-F}: 132.01 ± 41.24 seconds). This latency was significantly increased in App^{NL-F} on the fifth trial,
428 compared to the same genotype on the first trial ($p<0.01$). Together, these results show an intact
429 social memory in App^{NL-F} mice at six months, and suggest a lack of motivation.

430 To rule out that potential olfactory dysfunctions, which could interfere with the social memory
431 tests, we performed an olfactory habituation/dishabituation test ([38]; **figure 4E**). Four odors were
432 tested and showed no significant differences between C57Bl6 and App^{NL-F} mice. Both strains spent
433 more times interacting with social odors, especially from an unknown cage, showing (1) the absence
434 of olfactory problem and (2) the capacity of App^{NL-F} mice to discriminate social and non-social odors.
435

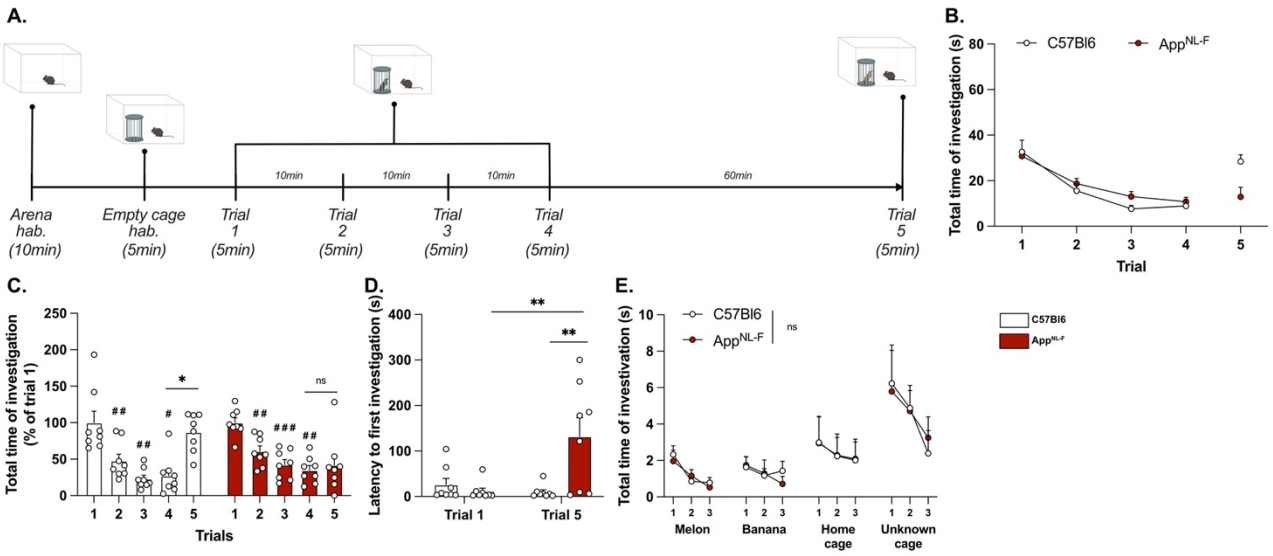

Figure 4 *: App^{NL-F} mice have no social memory deficits at six months old.*

*In the five-trials social memory test (A.), App^{NL-F} mice show no memory deficits as seen by the progressive decrease in social interactions over four consecutive trials (B.). On the fifth trial, when a new animal is presented, C57Bl6 mice regain interest whereas App^{NL-F} mice don't (C.). Latency to first investigation (D.) is similar between genotypes in the first trial. However, it is significantly increased in App^{NL-F} on the fifth trial. Two-way ANOVA for repeated measured with the genotype and the trial as the main factors. Bonferroni multiple comparison #, p<0.03, ##, p<0.01, ###, p<0.001: statistically different from trial 1; Bonferroni multiple comparison: **, p<0.01: statistically different as shown. C57Bl6: n=8, App^{NL-F}: n=8.*

In the olfactory habituation/dishabituation test (E.), we presented four different odors for three times two minutes each. No olfactory problems were unveiled. C57Bl6: n=9, App^{NL-F}: n=10.

450 *3.5. App^{NL-F} mice show a mild anxiety-/depression-like behavior.*

451 Early emotion related behaviors are still poorly described in Alzheimer's disease and has not
452 been the focus of experimental work. However, our results show that six months old App^{NL-F} mice do
453 not present social memory impairments, but a higher level of apathy (i.e., loss of interest for a task),
454 which is consistent with clinical studies [40] and prompted further research of emotional symptoms.

455 In the open field test, App^{NL-F} animals had a reduced locomotion as seen by the significant
456 reduction of the travelled distance (C57Bl6: 5663 ± 421.1 cm, App^{NL-F}: 3543 ± 61.1 cm; **figure 5A**)
457 in the arena ($p<0.01$), consistent with a previous report [41]. A deeper analysis of the behavior
458 revealed a significantly reduced number of entries (C57Bl6: 30.75 ± 4 entries, App^{NL-F}: 6.50 ± 1
459 entries) in the central area (**figure 5B**; $p<0.01$) whereas the time spent in that zone (C57Bl6: 81.16
460 ± 6.23 seconds, App^{NL-F}: 82.30 ± 7.22 seconds) remained the same (**figure 5C**). This suggests a
461 slightly higher anxiety-like state in App^{NL-F} animals, compared to C57Bl6 controls. To better
462 understand this behavior, the elevated plus maze was used [32, 42]. The number of entries (C57Bl6:
463 6.12 ± 1 entries, App^{NL-F}: 3.25 ± 1) in the open arms (anxiogenic area) was significantly reduced
464 ($p<0.05$; **figure 5D**) whereas the total time spent in this area (C57Bl6: 38.38 ± 5.68 seconds, App^{NL-}
465 ^{F}: 26.63 ± 5.76 seconds) was unchanged (**figure 5E**), confirming the higher emotional state.

466 We then explored the depression-like behavior in three different paradigms commonly used to
467 study emotions in rodent. In the forced swim test, the immobility (total time and latency to first) was
468 used as an indicator of resignation. The latency to the first immobility was significantly reduced in
469 App^{NL-F} (C57Bl6: 52.05 ± 0.30 seconds, App^{NL-F}: 25.43 ± 3.70 seconds, $p<0.05$; **figure 5F**) and the
470 total time of immobility was significantly increased in App^{NL-F} (C57Bl6: 48.07 ± 6.89 seconds, App^{NL-}
471 ^{F}: 90.07 ± 7.79 seconds; **figure 5G**; $p<0.001$) compared to C57Bl6 mice, characteristic of a
472 depression-like behavior. In the splash test, the lack of grooming reflects a lack of self-care. No
473 significant differences in the latency to first grooming (C57Bl6: 139.8 ± 17.46 seconds, App^{NL-F}: 108.1
474 ± 13.70 seconds; **figure 5H**), the frequency of grooming (C57Bl6: 6.60 ± 0.17, App^{NL-F}: 6.80 ± 0.37;
475 **figure 5I**) nor the total time of grooming (C57Bl6: 54.15 ± 9.81 seconds, App^{NL-F}: 68.98 ± 3.93
476 seconds; **figure 5J**) was observed in the App^{NL-F} mice compared to C57Bl6 mice. The sucrose
477 preference test, where a lack of preference for sugar compared to water is considered to reflect

478 anhedonia, revealed no difference between the two strains (C57Bl6: 103 ± 8.33 %, App^{NL-F}: 104 ±
479 3.80 %; **figure 5K**).
480 Lastly, the behavioral data related to anxiety- and depression-like phenotype were compiled into
481 an emotionality z-score [33]. We used several parameters per test to establish a test z-score
482 (ZSc_test; **supplementary table 1**) and each ZSc_test was then combined into an emotionality z-
483 score (**figure 5L**). The C57Bl6 mice were used as the control group and have an average z-score
484 close to zero (-0.05 ± .11). The App^{NL-F} mice had a significantly increased z-score (0.42 ± 0.13,
485 $p<0.01$) confirming an anxiety-/depression-like phenotype of App^{NL-F} mice at six months.
486

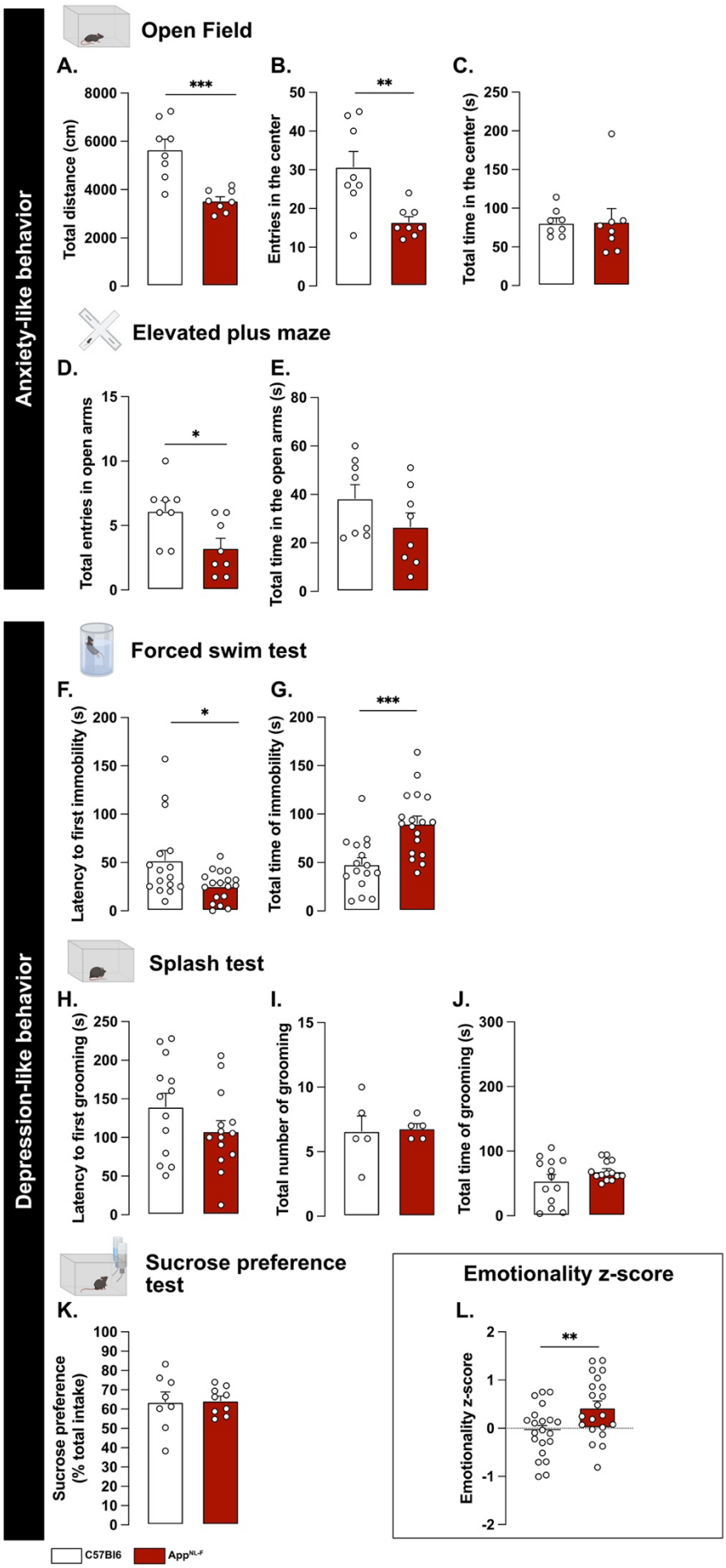
Anxiety-like behavior
Open Field
A.
Total distance (cm)
8000
6000
4000
2000
0
***
B.
Entries in the center
50
40
30
20
10
0
**
C.
Total time in the center (s)
250
200
150
100
50
0
Elevated plus maze
D.
Total entries in open arms
15
10
5
0
*
E.
Total time in the open arms (s)
80
60
40
20
0
Depression-like behavior
Forced swim test
F.
Latency to first immobility (s)
200
150
100
50
0
*
G.
Total time of immobility (s)
200
150
100
50
0
***
Splash test
H.
Latency to first grooming (s)
250
200
150
100
50
0
I.
Total number of grooming
15
10
5
0
J.
Total time of grooming (s)
300
200
100
0
Sucrose preference test
K.
Sucrose preference (% total intake)
100
90
80
70
60
50
40
30
20
10
0
Emotionality z-score
L.
Emotionality z-score
2
1
0
-1
-2
**
C57Bl6
App NL-F

487

488 ***<u>Figure 5</u> : App^{NL-F} mice display mild anxiety/depressive-like behavior.***

489 *In the open filed test, the total travelled distance (A.) is reduced in App^{NL-F} as well as the number of*
490 *entries in the central area (B.). The total time in that zone (C.) remains unchanged. Mann-Whitney*
491 *test: **, p<0.01, ***, p<0.001 statistically different as shown. C57Bl6: n=8, App^{NL-F}: n=8. In the*
492 *elevated plus maze, the number of entries in the open arms (D.) is significantly reduced whereas the*
493 *total time spent in the open arms (E.) remains unchanged between genotypes. Altogether, these*
494 *observations suggest a mild anxiety-like phenotype. Student t-test: *, p<0.05 statistically different as*
495 *shown. C57Bl6: n=8, App^{NL-F}: n=8.*

496 *In the forced swim test, the latency to first immobility (F.) is reduced in App^{NL-F} mice while the total*
497 *time of immobility (G.) is increased in these animals. This suggests a depression-like phenotype.*
498 *Mann-Whitney and student t-test: *, p<0.05, ***, p<0.001 statistically different as shown. C57Bl6:*
499 *n=16, App^{NL-F}: n=18. Our analysis does not unveil any difference in the latency to first grooming (H.),*
500 *total number of grooming (I.) nor in the total time of grooming (J.). C57Bl6: n=13, App^{NL-F}: n=14. For*
501 *the frequency n=4 and n=5 for C57Bl6 and App^{NL-F} respectively. No difference was unveiled in the*
502 *sucrose consumption measured in the sucrose preference test (K.) C57Bl6: n=8, App^{NL-F}: n=9.*

503 *The emotionality z-score (L.) is an integrative score allowing comparison of multiple factors,*
504 *calculated on different scales. It is used here to assess the anxiety-/depression-like state of our*
505 *animals and includes parameters from the different behavioral test above-mentioned. Our analysis*
506 *reveals an increased emotionality z-score in App^{NL-F} compared to C57Bl6 controls. This is the*
507 *reflection of a higher anxiety-/depression-like phenotype observed in these animals. Student t-test:*
508 ***, p<0.01 statistically significant as shown. C57Bl: n=21, App^{NL-F}: n=21.*

509

510 *3.6. Single injection of ketamine (5mg/kg) partially reverses synaptic hypersensitivity*.

511 In the light of the depression-like behavior in the App^{NL-F} mice, we asked whether an
512 antidepressant treatment would correct the behavior as well as the observed synaptic impairments.
513 The NMDA receptors antagonist ketamine is a rapid-acting antidepressant, and previous studies in
514 our lab has shown the long lasting retuning effect of this molecule in a rat model of depression [43].

515 Six months old App^{NL-F} mice received either ketamine (5mg/kg) or vehicle solution (NaCl 0.9%)
516 through i.p injections and acute hippocampal slices were prepared twenty-four hours after injection.
517 Patch-clamp recordings revealed no differences in the resting membrane potential (NaCl: -53.64 ±
518 3.08 mV, ketamine: -51.53 ± 5.29 mV; **figure 6A**) between the two groups, nor any difference in
519 sEPSC frequency (NaCl: 0.33 ± 0.11 Hz, ketamine: .43 ± 0.2 Hz; **figure 6B-D**), amplitude (NaCl: -
520 33.70 ± 5.42 pA, ketamine: -21.84 ± 2.69 pA; **figure 6C**), decay (**supplementary figure 2A**) or rise
521 time (**supplementary figure 2B**). However, we observed a significant increase of the frequency of
522 mEPSC (NaCl: 0.10 ± 0.001 Hz, ketamine: 0.59 ± 0.11 Hz, $p<0.01$; **figure 6E-D**). The amplitude
523 (NaCl: -29.03 ± 4.40 pA, ketamine: -21.89 ± 3.52 pA; **figure 6F**), decay (**supplementary figure 2C**)
524 and rise time (**supplementary figure 2D**) of mEPSC were not different between groups.

525 In the field recording experiment (**figure 6G-I**), the subthreshold θ-burst stimulation gave an initial
526 potentiation of the fEPSP in both conditions (**figure 6G-H**). The potentiation was maintained in App^{NL-}
527 ^{F} + NaCl mice, but not in the ketamine treated animals. One hour after the stimulation, the magnitude
528 of fEPSP was significantly increased compared to before the θ-burst stimulation. However, it was
529 significantly lower than in vehicle treated mice (**figure 6G-I**). Taken together, these electrophysiology
530 recordings confirm the ability of ketamine to retune misregulated synaptic transmission and plasticity.
531

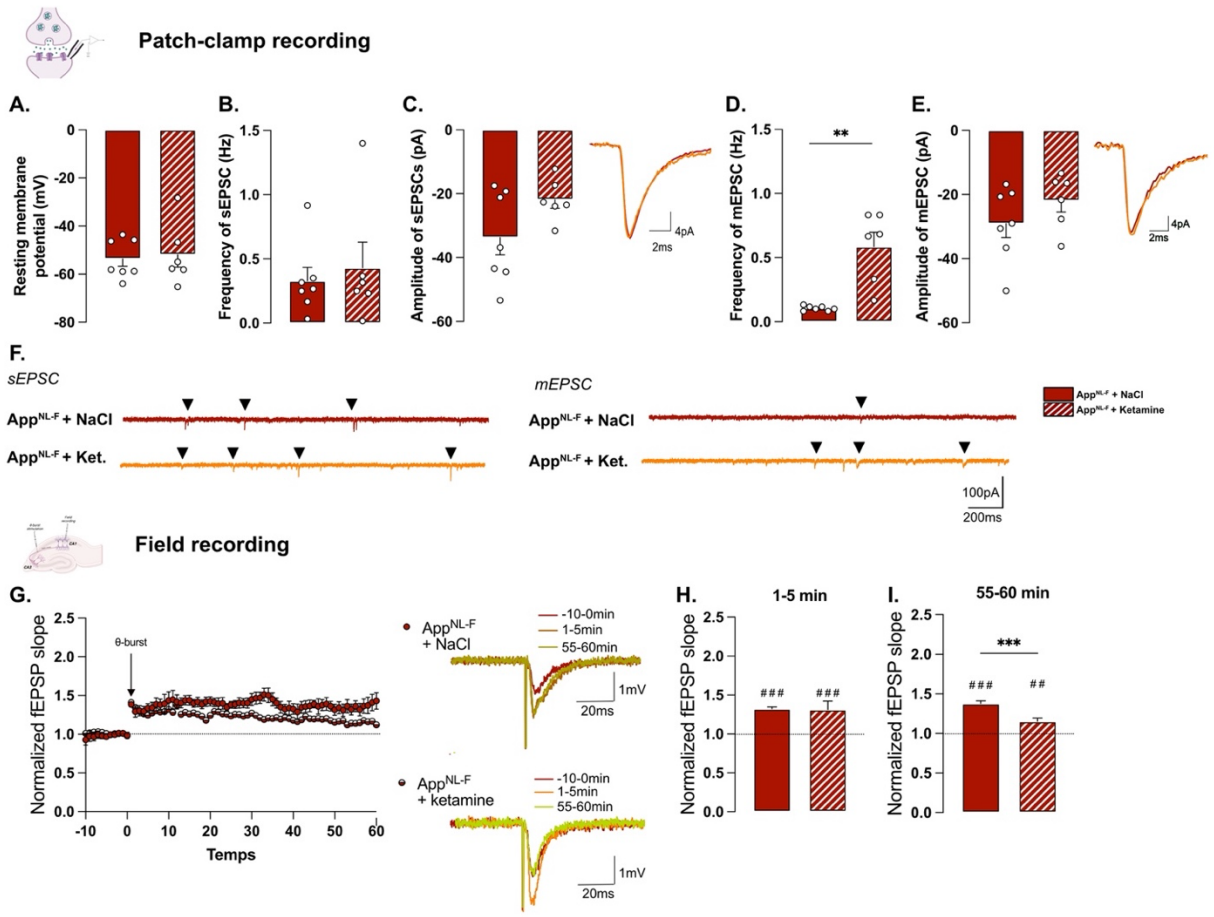

532

533

534 ***<u>Figure 6</u> : App^{NL-F} mice's synaptic mistuning is partially restored by ketamine 5mg/kg injection***

535 *Resting membrane potential (A.) is unchanged after ketamine treatment. Whilst the frequency (B.)*

536 *and the amplitude (C.) of the sEPSC are not different between treatments, the frequency of mEPSC*

537 *(D.) is increased in ketamine treated animals. The amplitude of mEPSC isunchanged. (F.) depicts*

538 *representative traces for both sEPSC and mEPSC. Mann-Whitney test: **, p<0.01 statistically*

539 *different as shown. From figure (A.) to (F.): App^{NL-F} + NaCl: n=7 cells recorded in five animals, App^{NL-}*

540 *^{F} + ketamine: n=6 cells recorded in six animals.*

541 *In the fEPSP experiment (G.), we used the same customized θ-burst stimulation protocol, which*

542 *elicites a potentiation (H.), in a similar fashion in both NaCl and ketamine treated animals. After one*

543 *hour (I.), the fEPSP goes back nearly to the baseline value whereas in the App^{NL-F} + NaCl the*

544 *stimulation triggers a long-term potentiation. Student t-test: ##, p<0.01, ###, p<0.001 statistically*

545 *different from 1; ***, p<0.001 statistically different as shown. App^{NL-F} + NaCl: n=5 recordings in four*

546 *animals, App^{NL-F} + ketamine: n=5 recordings in four animals.*

547

548 *3.7. Ketamine does not affect motivational problems in the five-trials social memory test.*

549 In the five-trials social memory test, no social memory impairments were unveiled in both
550 treatment conditions, as observed by the progressively decreasing time of social interactions over
551 the four first trials (**figure 7A**). In line with our previous experiments, the social interaction measured
552 in the fifth trial was not significantly different from the fourth trial in the vehicle treated animals (trial
553 4: 18.90 ± 4.66 % vs trial 5: 38.20 ± 5.91 %, **figure 7B**), confirming the apathy-like behavior.
554 Interestingly, ketamine didn't correct this behavior (trial 4: 22.085 ± 4.97 % vs. trial 5: 40.12 ± 9.48
555 %, **figure 7B**).

556

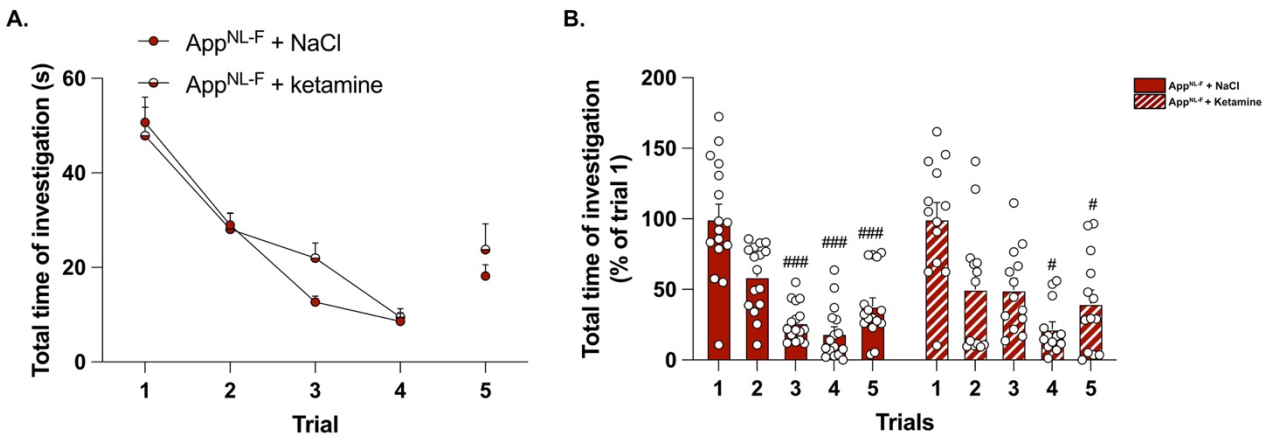

***<u>Figure 7</u>* : 5mg/kg ketamine doesn't affect motivational deficits in App^{NL-F} mice**

Whether treated with NaCl or ketamine, App^{NL-F} mice do not have social memory impairments (A.). On the fifth trial, the social interactions are not different from trial four neither from trial 1 (B.), suggesting a lack of motivation in App^{NL-F} mice. This lack of motivation is not corrected by 5mg/kg ketamine treatment. ANOVA de Friedman for repeated measure with treatment and trials as the main factors. Wilcoxon multiple comparison: #, $p<0.05$, ###, $p<0.001$ statistically different from trial 1. App^{NL-F} + NaCl: n=16, App^{NL-F} + ketamine: n=13.

567 *3.8. The antidepressant effect of ketamine partially restores the emotionality in six months old*
568 *App^{NL-F} mice.*

569 In the open field, none of the parameters total distance travelled (NaCl: 4331 ± 190.5 cm,
570 ketamine: 4454 ± 229.3 cm; **figure 8A**), the number of entries in the center (NaCl: 20.19 ± 2.30
571 entries, ketamine: 22.69 ± 2.55 entries; **figure 8B**) and total time spent in that zone (NaCl: 66.11 ±
572 6.35 seconds, ketamine: 83.13 ± 10.32 seconds; **figure 8C**) were changed by the ketamine
573 treatment. Likewise, ketamine had no effect on the elevated plus maze since there were no
574 differences between the groups in the number of entries in the open arms (NaCl: 0.87 ± 0.40 entries,
575 ketamine: 1.25 ± .25 entries; **figure 8D**) nor the total time spent in that zone (NaCl: 8.41 ± 3.2
576 seconds, ketamine: 1.12 ± 4.79 seconds; **figure 8E**).

577 In the forced swim test, no changes were observed in the latency to first immobility (NaCl: 20 ±
578 3.32 seconds, ketamine: 29.75 ± 6.56 seconds; **figure 8F**). However, there was a reduced total time
579 of immobility in ketamine treated mice compared to NaCl treated (NaCl: 114.4 ± 2.02 seconds,
580 ketamine: 71.88 ± 10.61, $p<0.05$; **figure 8G**). Similarly, in the splash test, a reduced latency to first
581 grooming (NaCl: 32.52 ± 3.71 seconds, ketamine: 16.30 ± 2.56 seconds, $p<0.01$; **figure 8H**),
582 increased frequency (NaCl: 7 ± 0.27, ketamine: 9.13 ± 0.69, $p<0.05$; **figure 8I**) and an increased
583 total time of grooming (NaCl: 145.7 ± 6.01 seconds, ketamine: 188.8 ± 3.56 seconds, $p<0.05$; **figure**
584 **8J**) were observed.

585 Finally, we integrated all these behavioral data into an emotional z-score (**figure 8K**) to assess
586 the overall effect of ketamine on the anxiety-/depression-like behavior of App^{NL-F}. Animals who
587 received the vehicle solution were used as the control group; Their emotionality z-score was close
588 to zero. Our analysis revealed no statistical difference in the z-score between the two different
589 groups. Although ketamine reversed several depression-like behaviors, we hypothesize that the
590 treatment used was perhaps not strong enough to significantly affect the z-score.
591

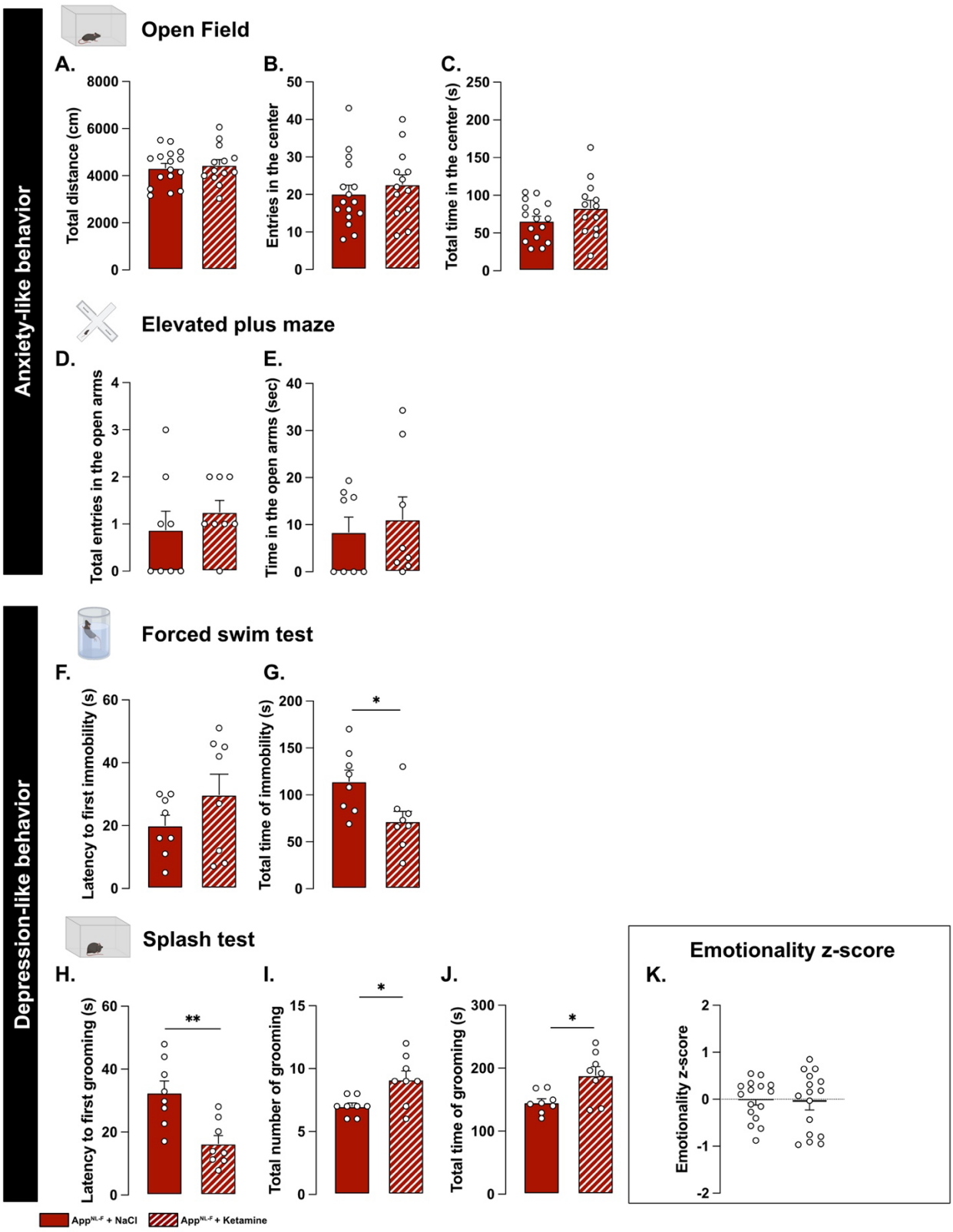
Anxiety-like behavior
Open Field
A.
Total distance (cm)
8000
6000
4000
2000
0
B.
Entries in the center
50
40
30
20
10
0
C.
Total time in the center (s)
250
200
150
100
50
0
Elevated plus maze
D.
Total entries in the open arms
4
3
2
1
0
E.
Time in the open arms (sec)
40
30
20
10
0
Depression-like behavior
Forced swim test
F.
Latency to first immobility (s)
60
40
20
0
G.
Total time of immobility (s)
200
150
100
50
0
*
Splash test
H.
Latency to first grooming (s)
60
40
20
0
**
I.
Total number of grooming
15
10
5
0
*
J.
Total time of grooming (s)
300
200
100
0
*
Emotionality z-score
K.
Emotionality z-score
2
1
0
-1
-2
App^NL-F + NaCl
App^NL-F + Ketamine

592

593

594 ***<u>Figure 8</u>* : Ketamine (5mg/kg) partially restores emotionality in six months old App^{NL-F} mice.**

595 *In the open filed test, neither the total travelled distance (A.), the number of entries in the central*
596 *area (B.) nor the total time in that zone (C.) is affected by ketamine. App^{NL-F} + NaCl: n=16, App^{NL-F} +*
597 *ketamine: n=13. A similar profile was obtained in the elevated plus maze in which both the number*
598 *of entries in the open arms (D.) and the total time in that zone (E.) are not affected. App^{NL-F} + NaCl:*
599 *n=8, App^{NL-F} + ketamine: n=8.*

600 *In the forced swim test, the latency to first immobility (F.) is unchanged after ketamine treatment*
601 *while the total time of immobility (G.) is reduced. This suggests an antidepressant effect of ketamine.*
602 *Student t-test: *, $p<0.05$ statistically different as shown. App^{NL-F} + NaCl: n=8, App^{NL-F} + ketamine:*
603 *n=8. Our analysis also unveils statistical difference in the latency to first grooming (H.), total number*
604 *of grooming (I.) and in the total time of grooming (J.). Student t-test: *, $p<0.05$, **, $p<0.01$ statistically*
605 *different as shown. App^{NL-F} + NaCl: n=8, App^{NL-F} + ketamine: n=8. Interestingly, the emotionality z-*
606 *score (K.) remains unchanged after ketamine 5mg/kg treatment. App^{NL-F} + NaCl: n=16, App^{NL-F} +*
607 *ketamine: n=16.*

608

609 **4. DISCUSSION**

610 As the final product of the dysregulated amyloid cascade, large Aβ plaques has traditionally been
611 studied as one of the main cause of Alzheimer's pathology [44], but this chain of events is now being
612 questioned. In six months old App^{NL-F} mice, Aβ plaques were not detectable with conventional
613 immunohistochemistry methods, although we see a slight increase in non-soluble Aβ concentrations
614 in the hippocampus. This was accompanied with early synaptic misfunction. In a late onset mouse
615 model of Alzheimer's disease (App^{NL-F}), we observed reduced synaptic activity and reduced
616 threshold to long-term potentiation in the hippocampus, associated with an early depression-like
617 behavior in six months old animals. Interestingly, these animals do not display social memory
618 impairments, but show apathy-like behavior, consistent with clinical reports [45]. Moreover, the
619 NMDA receptor antagonist ketamine, successfully increased the synaptic activity, and partially
620 restored the impaired plasticity, as suggested by previous work in our lab [35]. In good agreement,
621 we show the antidepressant effect of a low dose of ketamine [46] in our animal model of Alzheimer's
622 disease.

623 A reduced membrane potential and a reduced frequency of mEPSC in App^{NL-F} mice compared
624 to control are both signs of neuronal unhealthiness. This observation is consistent with previous
625 recordings obtained from primary neuronal cultures from the same line of mice, where reduced
626 synaptic functions was linked to reduced mitochondrial functions [34]. In fact, mitochondrial
627 dysfunction is a consistent phenomenon in early stages of Alzheimer's disease and reduced
628 mitochondrial activity would impair membrane potential as well as presynaptic release probability
629 since these are energy consuming processes [47-50]. Indeed, cell cultures from App^{NL-F} mice have
630 increased level of the aggregated prone Aβ42 form, together with impaired mitochondrial functions
631 and reduced presynaptic probability of release [34]. This study does not discriminate Aβ alloforms
632 (i.e., Aβ40 and Aβ42), however we do observe an increased concentration of aggregated Aβ in
633 homogenates of hippocampus and the cortex of six months old App^{NL-F} mice.

634 A decrease in mEPSC frequency is typically explained by a decreased probability of release at
635 the presynaptic terminal. Reduced synaptic transmission is frequently seen in Alzheimer's disease
636 [25] and presynaptic release has been suggested as a target for treatment [51]. It should be noted
637 however, that an opposite effect has also been observed [52]. In our work, a possible lower

638 probability of glutamate release, is accompanied with an unexpected reduced threshold for LTP.
639 Interestingly, western-blot analysis showed that App^{NL-F} mice express higher levels of the NMDA
640 receptor subunit GluN2A. This subunit is the most dynamic and essential in LTP induction [53], thus
641 providing a plausible mechanism for the lowered threshold for plasticity.

642 Cognitive impairment and memory loss is traditionally associated with reduced plasticity, and
643 previous work in the App^{NL-F} mice at six months old show no effect on LTP after a strong tetanic
644 stimulation [52]. Synaptic potentiation is however not linearly correlated with memory, rather synaptic
645 strength is constantly adjusted based on activity patterns in the neuronal network [54]. In order to
646 learn and adapt to the changing environment, synaptic transmission needs to be plastic, while
647 keeping the overall activity within optimal range. In fact, it has been proposed that cognitive deficits
648 in early Alzheimer's disease is not about reduced plasticity, but an imbalance at the network level
649 [55], which is compatible with a reduced threshold for potentiation. Interestingly, we also have
650 observed a reduced threshold for plasticity in other models with memory impairments [26, 35].

651 Our behavioral analysis revealed no social memory impairments, emphasizing the absence of
652 memory impairment at early stages of the pathology in App^{NL-F} animals [37, 41, 56]. Our experiments
653 do not exclude a lack of sociability, a commonly observed symptom in Alzheimer's patients [57, 58],
654 and described as altered in other animal models [38]. In contrast, App^{NL-F} showed mild anxiety-
655 /depression-like behavior at six months old, measured in several paradigms. This is in line with early
656 depressive symptoms observed in Alzheimer's patients [59] as well as in animals model of the
657 pathology [60, 61]. Additionally, we report, a decreased mobility in the open field, consistent with
658 previous report [41] (yet in contrast with the usually observed hyperactivity in other mouse model of
659 the pathology [62-65]).

660 Depression being described as a syndrome (i.e., a pathology gathering multiple symptoms), the
661 use of one unique test cannot, by itself, explain the effect of a genotype nor of a therapeutic strategy
662 on the behavior [66]. To get thus an overall vision of the emotional state of the App^{NL-F} mice, we
663 compiled our behavioral data into an emotionality z-score [33] relevant to study depression-like
664 behaviors assessed on different scales [32, 67]. Since reduced mobility could confound several of
665 the tests used to assess depression-like behavior, normalization of the different data obtained in the
666 open field and elevated plus maze with the travelled distance, compensating the lack of mobility.

667 Finally, we investigated the therapeutic effect of a low dose of ketamine (5mg/kg) delivered i.p,
668 twenty-four hours prior to experiments. At this dose, this NMDA receptor antagonist has a fast acting
669 antidepressant effect [46] in depressed patients [68, 69], rats [70, 71] and mice [72, 73]. In line with
670 the literature, we successfully show the antidepressant effect of this drug in the forced swim test and
671 the splash test. However, the overall emotionality z-score was not significantly improved. The
672 mechanism of action of ketamine is still debated, and a role of ketamine metabolites rather than
673 ketamine itself, has been proposed [74-77]. In particular, norketamine and hydroxynorketamine [78]
674 both induce sustainable antidepressant effect [73]. In contrast to their high efficacy [73, 79], these
675 metabolites have a low availability [80]. This very low bioavailability, yet of a very active compound,
676 would be an explanation for the partial antidepressant effect of ketamine.

677 An alternative mechanism of action is that ketamine restores and stabilizes synaptic transmission
678 [43]. We have previously shown an acute effect of ketamine on LTP threshold when applied to
679 hippocampal brain slices [35].This is in good agreement with the present data where systemic
680 ketamine increased the frequency of mEPSC to a similar level to the one observed in C57Bl6
681 controls, and restored the threshold to trigger LTP after a subthreshold stimulation of Schaffer
682 collaterals. Hence, the antidepressant effect of ketamine can be explained by an acute blocking of
683 NMDA receptors, stabilizing synaptic activity [81].

684 Acute treatment of ketamine appears promising to treat the early depressive symptoms of
685 Alzheimer's disease. Interestingly, increasing synchronous neuronal activity in the gamma frequency
686 has been shown to slow-down disease progress and improve cognitive performance [82], although
687 these results have been challenged [83]. Restoring synaptic transmission and plasticity may be a
688 biological mechanism underlying the beneficial effect of a mental and physical active life-style [84]
689 and could have a prophylactic effect. The effect of chronic ketamine treatment on Alzheimer's
690 disease progression would thus be interesting to follow-up.

691 Research for Alzheimer disease treatment has focused mainly on Aβ reducing treatments [85,
692 86] or the cholinergic system [87, 88]. Here we show that early synaptic impairment as well as early
693 depression-like behaviors observed in an Alzheimer's disease model can be partially corrected by
694 pharmacological intervention targeting the glutamatergic system. This may explain why treatments

695 that reduce Aβ load are only moderately effective in treating cognitive symptoms [89-91], and should
696 be carefully considered when developing new therapeutic strategies.
697
698 **AUTHOR CONTRIBUTION**
699 Conceptualization M.L and P.N, Investigation B.P, M.S, T.P.B and N.M, Supervision G.H and M.L.
700 Writing the original draft preparation B.P., N.M and M.L; funding acquisition B.P and M.L.
701
702 **INSTITUTIONAL REVIEW BOARD STATEMENT**
703 The study was conduct in accordance with the Declaration of Helsinki and was approved by the
704 Swedish board of animal use (Jordbruksverket ethical permit #5.2.18-03389/2020) and accepted by
705 the ethics committee at Uppsala University (Djurskyddsorganet at Uppsala University, accreditation
706 #DOUU-2020-022).
707
708 **FUNDING**
709 This work was supported by the Swedish Alzheimer's Foundation (to M.L.), Wenner-Gren Stiftelsen
710 (to M.L), O.E Edla Johansson Vetenskapliga stiftelsen (to B.P.) and Gun och Bertils Stohnes
711 stiftelsen (to B.P).
712
713 **ACKNOWLEDGMENTS**
714 The authors would like to thank both the BioVis imaging facility and the Uppsala University
715 Behavioral Facility (UUBF) for their expertise and their help on setting up the different experiments.
716
717 **CONFLICTS OF INTEREST**
718 All the cartoons were created with BioRender.com.
719 The authors declare no conflict of interest.
720
721 **REFERENCES**
722 1. Ferri, C.P., et al., *World Alzheimer's report 2009*, in *Alzheimer's disease international*, M.
723 Prince and J. Jackson, Editors. 2009.

724 2. Jahn, H., *Memory loss in Alzheimer's disease.* Dialogues Clin Neurosci, 2013. **15**(4): p. 445-
725 54.
726 3. Shen, L.X., et al., *Social Isolation, Social Interaction, and Alzheimer's Disease: A Mendelian*
727 *Randomization Study.* J Alzheimers Dis, 2021. **80**(2): p. 665-672.
728 4. Zubenko, G.S., et al., *A collaborative study of the emergence and clinical features of the*
729 *major depressive syndrome of Alzheimer's disease.* Am J Psychiatry, 2003. **160**(5): p. 857-
730 66.
731 5. Naseri, N.N., et al., *The complexity of tau in Alzheimer's disease.* Neurosci Lett, 2019. **705**:
732 p. 183-194.
733 6. O'Brien, R.J. and P.C. Wong, *Amyloid precursor protein processing and Alzheimer's disease.*
734 Annu Rev Neurosci, 2011. **34**: p. 185-204.
735 7. Soria Lopez, J.A., H.M. Gonzalez, and G.C. Leger, *Alzheimer's disease.* Handb Clin Neurol,
736 2019. **167**: p. 231-255.
737 8. Damoiseaux, J.S., *Effects of aging on functional and structural brain connectivity.*
738 Neuroimage, 2017. **160**: p. 32-40.
739 9. Wyss-Coray, T., *Ageing, neurodegeneration and brain rejuvenation.* Nature, 2016.
740 **539**(7628): p. 180-186.
741 10. Elobeid, A., et al., *Altered Proteins in the Aging Brain.* J Neuropathol Exp Neurol, 2016. **75**(4):
742 p. 316-25.
743 11. Busche, M.A., et al., *Clusters of hyperactive neurons near amyloid plaques in a mouse model*
744 *of Alzheimer's disease.* Science, 2008. **321**(5896): p. 1686-9.
745 12. Siskova, Z., et al., *Dendritic structural degeneration is functionally linked to cellular*
746 *hyperexcitability in a mouse model of Alzheimer's disease.* Neuron, 2014. **84**(5): p. 1023-33.
747 13. Frisoni, G.B., et al., *The probabilistic model of Alzheimer disease: the amyloid hypothesis*
748 *revised.* Nat Rev Neurosci, 2022. **23**(1): p. 53-66.
749 14. Petrache, A.L., et al., *Aberrant Excitatory-Inhibitory Synaptic Mechanisms in Entorhinal*
750 *Cortex Microcircuits During the Pathogenesis of Alzheimer's Disease.* Cereb Cortex, 2019.
751 **29**(4): p. 1834-1850.

752 15. Castellani, R.J., G. Plascencia-Villa, and G. Perry, *The amyloid cascade and Alzheimer's*
753 *disease therapeutics: theory versus observation.* Lab Invest, 2019. **99**(7): p. 958-970.
754 16. Bateman, R.J., N.R. Barthelemy, and K. Horie, *Another step forward in blood-based*
755 *diagnostics for Alzheimer's disease.* Nat Med, 2020. **26**(3): p. 314-316.
756 17. Koch, G. and D. Spampinato, *Alzheimer disease and neuroplasticity.* Handb Clin Neurol,
757 2022. **184**: p. 473-479.
758 18. Styr, B. and I. Slutsky, *Imbalance between firing homeostasis and synaptic plasticity drives*
759 *early-phase Alzheimer's disease.* Nat Neurosci, 2018. **21**(4): p. 463-473.
760 19. Lyketsos, C.G., et al., *Neuropsychiatric symptoms in Alzheimer's disease.* Alzheimers
761 Dement, 2011. **7**(5): p. 532-9.
762 20. Wolinsky, D., K. Drake, and J. Bostwick, *Diagnosis and Management of Neuropsychiatric*
763 *Symptoms in Alzheimer's Disease.* Curr Psychiatry Rep, 2018. **20**(12): p. 117.
764 21. van Dyck, C.H., et al., *Lecanemab in Early Alzheimer's Disease.* N Engl J Med, 2023. **388**(1):
765 p. 9-21.
766 22. Gustavsson, T., et al., *Long-term effects of immunotherapy with a brain penetrating Abeta*
767 *antibody in a mouse model of Alzheimer's disease.* Alzheimers Res Ther, 2023. **15**(1): p. 90.
768 23. Esquerda-Canals, G., et al., *Mouse Models of Alzheimer's Disease.* J Alzheimers Dis, 2017.
769 **57**(4): p. 1171-1183.
770 24. Sasaguri, H., et al., *APP mouse models for Alzheimer's disease preclinical studies.* EMBO J,
771 2017. **36**(17): p. 2473-2487.
772 25. Arroyo-Garcia, L.E., et al., *Impaired spike-gamma coupling of area CA3 fast-spiking*
773 *interneurons as the earliest functional impairment in the App(NL-G-F) mouse model of*
774 *Alzheimer's disease.* Mol Psychiatry, 2021. **26**(10): p. 5557-5567.
775 26. Loera-Valencia, R., et al., *High levels of 27-hydroxycholesterol results in synaptic plasticity*
776 *alterations in the hippocampus.* Sci Rep, 2021. **11**(1): p. 3736.
777 27. Saito, T., et al., *Single App knock-in mouse models of Alzheimer's disease.* Nat Neurosci,
778 2014. **17**(5): p. 661-3.
779 28. Nilsson, P., T. Saito, and T.C. Saido, *New mouse model of Alzheimer's.* ACS Chem Neurosci,
780 2014. **5**(7): p. 499-502.

29. Jiang, R., et al., *Autophagy Impairment in App Knock-in Alzheimer's Model Mice.* Front Aging Neurosci, 2022. **14**: p. 878303.

30. Leal, N.S., et al., *Amyloid Beta-Peptide Increases Mitochondria-Endoplasmic Reticulum Contact Altering Mitochondrial Function and Autophagosome Formation in Alzheimer's Disease-Related Models.* Cells, 2020. **9**(12).

31. Park, M. and K. Shen, *WNTs in synapse formation and neuronal circuitry.* EMBO J, 2012. **31**(12): p. 2697-704.

32. Quesseveur, G., et al., *Attenuated Levels of Hippocampal Connexin 43 and its Phosphorylation Correlate with Antidepressant- and Anxiolytic-Like Activities in Mice.* Front Cell Neurosci, 2015. **9**: p. 490.

33. Guilloux, J.P., et al., *Integrated behavioral z-scoring increases the sensitivity and reliability of behavioral phenotyping in mice: relevance to emotionality and sex.* J Neurosci Methods, 2011. **197**(1): p. 21-31.

34. Dentoni, G., et al., *Mitochondrial Alterations in Neurons Derived from the Murine AppNL-F Knock-In Model of Alzheimer's Disease.* J Alzheimers Dis, 2022. **90**(2): p. 565-583.

35. Juarez, E.V., I. Srivastava, and M. Lindskog, *Impaired glutamate reuptake induces synaptic mistuning in rat hippocampal slices, that can be counteracted by ketamine.* BioRxiv, 2022(2022.2001.2025.477658).

36. Shipton, O.A. and O. Paulsen, *GluN2A and GluN2B subunit-containing NMDA receptors in hippocampal plasticity.* Philos Trans R Soc Lond B Biol Sci, 2014. **369**(1633): p. 20130163.

37. Britz, J., et al., *Assessing Sex-Specific Circadian, Metabolic, and Cognitive Phenotypes in the AbetaPP/PS1 and APPNL-F/NL-F Models of Alzheimer's Disease.* J Alzheimers Dis, 2022. **85**(3): p. 1077-1093.

38. Rey, C.C., et al., *Altered inhibitory function in hippocampal CA2 contributes in social memory deficits in Alzheimer's mouse model.* iScience, 2022. **25**(3): p. 103895.

39. Fratiglioni, L., et al., *Influence of social network on occurrence of dementia: a community-based longitudinal study.* Lancet, 2000. **355**(9212): p. 1315-9.

40. Deardorff, W.J. and G.T. Grossberg, *Behavioral and psychological symptoms in Alzheimer's dementia and vascular dementia.* Handb Clin Neurol, 2019. **165**: p. 5-32.

810 41. Aladeokin, A.C., et al., *Network-guided analysis of hippocampal proteome identifies novel*
811 *proteins that colocalize with Abeta in a mice model of early-stage Alzheimer's disease.*
812 Neurobiol Dis, 2019. **132**: p. 104603.
813 42. Carobrez, A.P. and L.J. Bertoglio, *Ethological and temporal analyses of anxiety-like behavior:*
814 *the elevated plus-maze model 20 years on.* Neurosci Biobehav Rev, 2005. **29**(8): p. 1193-
815 205.
816 43. Juarez, E.V., I. Srivastava, and M. Lindskog, *Impaired glutamate reuptake induces synaptic*
817 *mistuning in rat hippocampal slices, that can be counteracted by ketamine.* BioRxiv,
818 2022(2022.2001.2025.477658).
819 44. Selkoe, D.J. and J. Hardy, *The amyloid hypothesis of Alzheimer's disease at 25 years.* EMBO
820 Mol Med, 2016. **8**(6): p. 595-608.
821 45. Vergallo, A., et al., *Association Between CSF Beta-Amyloid and Apathy in Early-Stage*
822 *Alzheimer Disease.* J Geriatr Psychiatry Neurol, 2019. **32**(3): p. 164-169.
823 46. Pham, T.H. and A.M. Gardier, *Fast-acting antidepressant activity of ketamine: highlights on*
824 *brain serotonin, glutamate, and GABA neurotransmission in preclinical studies.* Pharmacol
825 Ther, 2019. **199**: p. 58-90.
826 47. Calkins, M.J. and P.H. Reddy, *Amyloid beta impairs mitochondrial anterograde transport and*
827 *degenerates synapses in Alzheimer's disease neurons.* Biochim Biophys Acta, 2011.
828 **1812**(4): p. 507-13.
829 48. Reddy, P.H. and M.F. Beal, *Amyloid beta, mitochondrial dysfunction and synaptic damage:*
830 *implications for cognitive decline in aging and Alzheimer's disease.* Trends Mol Med, 2008.
831 **14**(2): p. 45-53.
832 49. Guo, L., J. Tian, and H. Du, *Mitochondrial Dysfunction and Synaptic Transmission Failure in*
833 *Alzheimer's Disease.* J Alzheimers Dis, 2017. **57**(4): p. 1071-1086.
834 50. Verma, M., B.N. Lizama, and C.T. Chu, *Excitotoxicity, calcium and mitochondria: a triad in*
835 *synaptic neurodegeneration.* Transl Neurodegener, 2022. **11**(1): p. 3.
836 51. Bliss, T.V. and G.L. Collingridge, *Expression of NMDA receptor-dependent LTP in the*
837 *hippocampus: bridging the divide.* Mol Brain, 2013. **6**: p. 5.

838 52. Benitez, D.P., et al., *Knock-in models related to Alzheimer's disease: synaptic transmission,*
839 *plaques and the role of microglia.* Mol Neurodegener, 2021. **16**(1): p. 47.
840 53. Paoletti, P., C. Bellone, and Q. Zhou, *NMDA receptor subunit diversity: impact on receptor*
841 *properties, synaptic plasticity and disease.* Nat Rev Neurosci, 2013. **14**(6): p. 383-400.
842 54. Neves, G., S.F. Cooke, and T.V. Bliss, *Synaptic plasticity, memory and the hippocampus: a*
843 *neural network approach to causality.* Nat Rev Neurosci, 2008. **9**(1): p. 65-75.
844 55. Frere, S. and I. Slutsky, *Alzheimer's Disease: From Firing Instability to Homeostasis Network*
845 *Collapse.* Neuron, 2018. **97**(1): p. 32-58.
846 56. Masuda, A., et al., *Cognitive deficits in single App knock-in mouse models.* Neurobiol Learn
847 Mem, 2016. **135**: p. 73-82.
848 57. Frisoni, G.B., et al., *Behavioral syndromes in Alzheimer's disease: description and correlates.*
849 Dement Geriatr Cogn Disord, 1999. **10**(2): p. 130-8.
850 58. Ballard, C., et al., *Alzheimer's disease.* Lancet, 2011. **377**(9770): p. 1019-31.
851 59. Enache, D., B. Winblad, and D. Aarsland, *Depression in dementia: epidemiology,*
852 *mechanisms, and treatment.* Curr Opin Psychiatry, 2011. **24**(6): p. 461-72.
853 60. Yan, L., et al., *Age-related neuropsychiatric symptoms in presenilins conditional double*
854 *knockout mice.* Brain Res Bull, 2013. **97**: p. 104-11.
855 61. Patel, S., et al., *Cotinine halts the advance of Alzheimer's disease-like pathology and*
856 *associated depressive-like behavior in Tg6799 mice.* Front Aging Neurosci, 2014. **6**: p. 162.
857 62. Moechars, D., et al., *Early phenotypic changes in transgenic mice that overexpress different*
858 *mutants of amyloid precursor protein in brain.* J Biol Chem, 1999. **274**(10): p. 6483-92.
859 63. Filali, M., R. Lalonde, and S. Rivest, *Anomalies in social behaviors and exploratory activities*
860 *in an APPswe/PS1 mouse model of Alzheimer's disease.* Physiol Behav, 2011. **104**(5): p.
861 880-5.
862 64. Toda, T., et al., *Presenilin-2 mutation causes early amyloid accumulation and memory*
863 *impairment in a transgenic mouse model of Alzheimer's disease.* J Biomed Biotechnol, 2011.
864 **2011**: p. 617974.
865 65. Cheng, D., et al., *Novel behavioural characteristics of the APP(Swe)/PS1DeltaE9 transgenic*
866 *mouse model of Alzheimer's disease.* Behav Brain Res, 2013. **245**: p. 120-7.

867 66. Soderlund, J. and M. Lindskog, *Relevance of Rodent Models of Depression in Clinical*
868 *Practice: Can We Overcome the Obstacles in Translational Neuropsychiatry?* Int J
869 Neuropsychopharmacol, 2018. **21**(7): p. 668-676.
870 67. Portal, B., et al., *Astroglial Connexins Inactivation Increases Relapse of Depressive-like*
871 *Phenotype after Antidepressant Withdrawal.* Int J Mol Sci, 2022. **23**(21).
872 68. Newport, D.J., et al., *Ketamine and Other NMDA Antagonists: Early Clinical Trials and*
873 *Possible Mechanisms in Depression.* Am J Psychiatry, 2015. **172**(10): p. 950-66.
874 69. Xu, Y., et al., *Effects of Low-Dose and Very Low-Dose Ketamine among Patients with Major*
875 *Depression: a Systematic Review and Meta-Analysis.* Int J Neuropsychopharmacol, 2016.
876 **19**(4).
877 70. Moghaddam, B., et al., *Activation of glutamatergic neurotransmission by ketamine: a novel*
878 *step in the pathway from NMDA receptor blockade to dopaminergic and cognitive disruptions*
879 *associated with the prefrontal cortex.* J Neurosci, 1997. **17**(8): p. 2921-7.
880 71. Li, N., et al., *mTOR-dependent synapse formation underlies the rapid antidepressant effects*
881 *of NMDA antagonists.* Science, 2010. **329**(5994): p. 959-64.
882 72. Brachman, R.A., et al., *Ketamine as a Prophylactic Against Stress-Induced Depressive-like*
883 *Behavior.* Biol Psychiatry, 2016. **79**(9): p. 776-786.
884 73. Pham, T.H., et al., *Common Neurotransmission Recruited in (R,S)-Ketamine and (2R,6R)-*
885 *Hydroxynorketamine-Induced Sustained Antidepressant-like Effects.* Biol Psychiatry, 2018.
886 **84**(1): p. e3-e6.
887 74. Adams, J.D., Jr., et al., *Studies on the biotransformation of ketamine. 1-Identification of*
888 *metabolites produced in vitro from rat liver microsomal preparations.* Biomed Mass Spectrom,
889 1981. **8**(11): p. 527-38.
890 75. Chang, T. and A.J. Glazko, *Biotransformation and disposition of ketamine.* Int Anesthesiol
891 Clin, 1974. **12**(2): p. 157-77.
892 76. Moaddel, R., et al., *A parallel chiral-achiral liquid chromatographic method for the*
893 *determination of the stereoisomers of ketamine and ketamine metabolites in the plasma and*
894 *urine of patients with complex regional pain syndrome.* Talanta, 2010. **82**(5): p. 1892-904.

895 77. Woolf, T.F. and J.D. Adams, *Biotransformation of ketamine, (Z)-6-hydroxyketamine, and (E)-*
896 *6-hydroxyketamine by rat, rabbit, and human liver microsomal preparations.* Xenobiotica,
897 1987. **17**(7): p. 839-47.
898 78. Chou, D., et al., *(2R,6R)-hydroxynorketamine rescues chronic stress-induced depression-*
899 *like behavior through its actions in the midbrain periaqueductal gray.* Neuropharmacology,
900 2018. **139**: p. 1-12.
901 79. Zanos, P., et al., *NMDAR inhibition-independent antidepressant actions of ketamine*
902 *metabolites.* Nature, 2016. **533**(7604): p. 481-6.
903 80. Highland, J.N., et al., *Mouse, rat, and dog bioavailability and mouse oral antidepressant*
904 *efficacy of (2R,6R)-hydroxynorketamine.* J Psychopharmacol, 2019. **33**(1): p. 12-24.
905 81. Autry, A.E., et al., *NMDA receptor blockade at rest triggers rapid behavioural antidepressant*
906 *responses.* Nature, 2011. **475**(7354): p. 91-5.
907 82. Martorell, A.J., et al., *Multi-sensory Gamma Stimulation Ameliorates Alzheimer's-Associated*
908 *Pathology and Improves Cognition.* Cell, 2019. **177**(2): p. 256-271 e22.
909 83. Soula, M., et al., *Forty-hertz light stimulation does not entrain native gamma oscillations in*
910 *Alzheimer's disease model mice.* Nat Neurosci, 2023. **26**(4): p. 570-578.
911 84. Janssen, N., et al., *Association Between Cognition, Health Related Quality of Life, and Costs*
912 *in a Population at Risk for Cognitive Decline.* J Alzheimers Dis, 2022. **89**(2): p. 623-632.
913 85. Sevigny, J., et al., *The antibody aducanumab reduces Abeta plaques in Alzheimer's disease.*
914 Nature, 2016. **537**(7618): p. 50-6.
915 86. Yang, P. and F. Sun, *Aducanumab: The first targeted Alzheimer's therapy.* Drug Discov Ther,
916 2021. **15**(3): p. 166-168.
917 87. Eldufani, J. and G. Blaise, *The role of acetylcholinesterase inhibitors such as neostigmine*
918 *and rivastigmine on chronic pain and cognitive function in aging: A review of recent clinical*
919 *applications.* Alzheimers Dement (N Y), 2019. **5**: p. 175-183.
920 88. Sharma, K., *Cholinesterase inhibitors as Alzheimer's therapeutics (Review).* Mol Med Rep,
921 2019. **20**(2): p. 1479-1487.
922 89. Salloway, S., et al., *Two phase 3 trials of bapineuzumab in mild-to-moderate Alzheimer's*
923 *disease.* N Engl J Med, 2014. **370**(4): p. 322-33.

924 90. Honig, L.S., et al., *Trial of Solanezumab for Mild Dementia Due to Alzheimer's Disease.* N
925 Engl J Med, 2018. **378**(4): p. 321-330.
926 91. Cummings, J.L., et al., *ABBY: A phase 2 randomized trial of crenezumab in mild to moderate*
927 *Alzheimer disease.* Neurology, 2018. **90**(21): p. e1889-e1897.
928